

Spectral Reflectance Estimation with Smoothness Constraint

Shoji Tominaga; Norwegian University of Science and Technology, Gjøvik, Norway / Nagano University, Ueda, Japan

Shogo Nishi; Osaka Electro-Communication University, Neyagawa, Japan

Ryo Ohtera; Kobe Institute of Computing, Kobe, Japan

Hideaki Sakai; Kyoto University, Kyoto, Japan

Abstract

We consider the problem of estimating surface-spectral reflectance with a smoothness constraint from image data. The total variation of a spectral reflectance over the visible wavelength range is defined as the measure of smoothness. A penalty on roughness, equivalent to smoothness, is added to the performance index to estimate the spectral reflectance functions. The optimal estimates of the spectral reflectance functions are determined to minimize a total cost function consisting of the estimation error and the roughness of the spectral functions. An RGB camera and multiple LED light sources are used to construct the multispectral image acquisition system. We model the observed images using spectral sensitivities, illuminant spectrum, unknown spectral reflectance, a gain parameter, and an additive noise term. The estimation algorithms are developed for the two estimation methods of PCA and LMMSE. The optimal estimators are derived based on the least-square criterion for PCA and the mean squared error minimization criterion for LMMSE. The feasibility of the proposed method is shown in an experiment using three mobile phone cameras. It is confirmed that the optimal estimators improve the accuracy for both original PCA and LMMSE estimators.

Introduction

Surface-spectral reflectances of natural objects like fruits, leaves, and woods in natural scenes and artificial ones like plastics, paints, papers, and ceramics are usually smooth in the visible wavelength range. Principal component analysis (PCA) is often performed to represent the spectral function shape using a small number of basis functions on the assumption that the spectral reflectance is smooth [1]-[3]. As a result, the low-dimensional linear model using the small number of basis functions is successfully applied to solving the color constancy problem [4]-[5] and estimating surface and illumination functions in a multiband vision system [6]. Surface-spectral reflectances of most objects can be represented with the use of five to seven basis functions.

Another approach to generate smooth spectral functions is to use a smoothness constraint. In fact, we may encounter the problem that the reflectance functions obtained are too jagged to be realistic. The total wavelength variation of reflectance functions, which mathematically means the square of derivative integrated over the visible range, can usually be defined as a measure of the smoothness. There were some discussions to find the smoothest reflectance functions with the least variation of reflectance functions under an illumination condition, which means the function that has maximum smoothness [7]-[9]. However, this approach is only successful in suppressing the spectral variation of reflectance functions. It does not necessarily minimize the estimation error of the spectral reflectances.

To date, many methods have been proposed for estimating the spectral reflectance of an object surface from image data (see [10]).

In the finite-dimensional modelling methods [11]-[14], spectral reflectance is approximated by a linear combination of a small number of basis functions via such an analysis method as PCA. The weighting coefficients in the linear combination are determined to minimize the squared error for the image data. The Wiener estimation methods [15]-[21] are based on a statistical approach, where the noise in the imaging system and a certain statistic of spectral reflectance are considered. The algorithm is derived by minimizing the estimation error. The Wiener estimation methods are known as the most common methods when the spectral sensitivity functions of the imaging system are known. Recently, an improved estimation method, called the linear minimum mean-square error (LMMSE) estimator, was proposed to estimate surface-spectral reflectance from the image data [10]. In this method, a linear estimator was derived in a more general form than the Wiener estimator. The derived LMMSE estimator has the advantage of being an unbiased estimator. It is verified theoretically that the estimation accuracy of the LMMSE estimator is better than that of the Wiener estimator.

In this paper, we consider the problem of estimating surface-spectral reflectance with a smoothness constraint from the image data. A penalty on the roughness of the spectral reflectance, which is equivalent to the smoothness constraint, is added to the performance index to estimate the spectral reflectance functions. The optimal estimates of the spectral reflectance functions are determined to minimize a total cost function consisting of the estimation error and the roughness of the spectral functions.

We suppose a multispectral image acquisition system in the visible range, where an RGB digital camera captures multiple images for the scene of an object under multiple light sources. The observed image data are described using the three spectral functions: camera spectral sensitivities, illuminant spectra, and unknown surface-spectral reflectance, also the two parameters of a gain and an additive noise term. These parameters are estimated in a separate way.

Under this observation model, we develop optimal algorithms to achieve the best performances for the two estimation methods of PCA and LMMSE. In addition, we show that the smoothness constraint effectively improves the estimation accuracy of the surface-spectral reflectance functions.

In the following, first, we describe the observation model based on a multispectral image acquisition system and define the smoothness constraint on spectral reflectance functions. Next, the optimal estimation algorithms are derived by minimizing the total cost function with the smoothness constraint. The least-squares method is used for PCA, and the mean squared error minimization method is used for LMMSE. Finally, the feasibility of the proposed estimation methods for spectral-reflectance estimation is confirmed in an experiment using different mobile phone cameras. The

estimation accuracies are compared with the originals of the PCA and LMMSE methods.

Observation Model and Smoothness Definition

A. Observation Model

Figure 1 shows a multispectral imaging system in the visible range. An RGB camera captures multiple images for the scene of an object under multiple light sources with different illuminant spectra. Let M be the number of light sources; hence, the total number of system outputs is $3M$ because the camera has three RGB channels. Let the number i denote the output number by the combination of m lights ($m=1, 2, \dots, M$) and c color channels ($c=1, 2, 3$), so that $i=1, 2, 3, \dots, 3M$. The observations y_i ($i=1, 2, \dots, 3M$) by the camera outputs are described as

$$y_i = g \int_{400}^{700} x(\lambda) e_m(\lambda) r_c(\lambda) d\lambda + n_i, \quad (1)$$

where $x(\lambda)$ is the surface-spectral reflectance of a target object, $e_m(\lambda)$ ($m=1, 2, \dots, M$) represent the spectral power distribution of the light sources, $r_c(\lambda)$ ($c=1, 2, 3$) denote the spectral sensitivity functions of the camera in the visible range (400–700 nm). Furthermore, n_i denotes the noise in the imaging system. We assume that n_i is the white noise with zero mean and the variance a , and is uncorrelated with $x(\lambda)$. Note that y_i represent the digital camera outputs, while $x(\lambda)$, $e_m(\lambda)$, and $r_c(\lambda)$ are physical quantities. The coefficient g in Eq. (1) is the weight used to convert the model outputs to the practical digital outputs, which is called the *gain parameter*. The parameter g is unique to the imaging system, which depends on the conditions of imaging system. This parameter can be determined separately using a white reference standard with known spectral reflectance (see [10]).

The spectral functions of reflectance, illuminants, and sensitivities are sampled at N wavelength points with equal intervals in the visible range and represented by N -dimensional column vectors as

$$\mathbf{x} = \begin{bmatrix} x(\lambda_1) \\ x(\lambda_2) \\ \vdots \\ x(\lambda_N) \end{bmatrix}, \quad \mathbf{e}_m = \begin{bmatrix} e_m(\lambda_1) \\ e_m(\lambda_2) \\ \vdots \\ e_m(\lambda_N) \end{bmatrix}, \quad \mathbf{r}_c = \begin{bmatrix} r_c(\lambda_1) \\ r_c(\lambda_2) \\ \vdots \\ r_c(\lambda_N) \end{bmatrix}, \quad (2)$$

where $m=1, 2, \dots, M$ and $c=1, 2, 3$.

The discrete representation of the observation model is then expressed in matrix form as follows:

$$\mathbf{y} = g\mathbf{A}\mathbf{x} + \mathbf{n}, \quad (3)$$

where

$$\mathbf{y} = \begin{bmatrix} y_1 \\ y_2 \\ \vdots \\ y_{3M} \end{bmatrix}, \quad \mathbf{A} = \begin{bmatrix} (\mathbf{e}_1 \cdot * \mathbf{r}_1)' \Delta\lambda / 2 \\ (\mathbf{e}_2 \cdot * \mathbf{r}_2)' \Delta\lambda \\ \vdots \\ (\mathbf{e}_M \cdot * \mathbf{r}_3)' \Delta\lambda / 2 \end{bmatrix}, \quad \mathbf{n} = \begin{bmatrix} n_1 \\ n_2 \\ \vdots \\ n_{3M} \end{bmatrix}. \quad (4)$$

The symbol $(\cdot *)$, superscript t , and $\Delta\lambda$ represent the elementwise multiplication, matrix transposition, and wavelength sampling interval, respectively. Therefore, \mathbf{A} is a $(3M\text{-by-}N)$ matrix defined by the illuminant spectra and the spectral sensitivities. The vector \mathbf{n} denotes the observation noise. When the spectral functions are sampled with $\Delta\lambda = 5$ in the range of 400–700 nm, the spectral functions are represented by 61-dimensional column vectors with $N=61$.

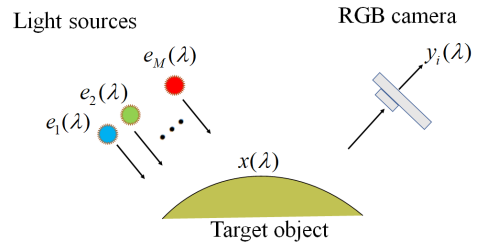


Figure 1 Observation model for the imaging system using an RGB camera.

B. Smoothness Definition

We can define the total variation of a spectral reflectance as a measure of smoothness, that is the square of its derivative, integrated over the entire visible range. Mathematically it is described as (see [7]):

$$\int_{400}^{700} (dx(\lambda)/d\lambda)^2 d\lambda. \quad (5)$$

We use the total variation as the smoothness constraint. The spectral reflectance function has maximum smoothness when the total variation is least, i.e., the smoothest. In this paper, we also use the term of roughness, which is the opposite of smoothness. The total variation corresponds to the roughness of the spectral reflectance function. The smoothest reflectance function is that function for which the total variation and so the roughness is least.

For convenience of numerical computation, the smoothness constraint is represented in discrete form using matrices. Firsts, the integration in Eq. (5) is approximated as

$$\int_{400}^{700} (dx(\lambda)/d\lambda)^2 d\lambda \approx \left\{ 0.5(dx(\lambda_1)/d\lambda)^2 + \sum_{i=2}^{N-1} (dx(\lambda_i)/d\lambda)^2 + 0.5(dx(\lambda_N)/d\lambda)^2 \right\} \Delta\lambda \quad (6)$$

Then, the discrete representation is given as [9]

$$\int_{400}^{700} (dx(\lambda)/d\lambda)^2 d\lambda \approx \|\mathbf{J}\mathbf{x}\|^2 / \Delta\lambda \quad (7)$$

where \mathbf{J} is a (N -by- N) matrix for the differentiation operator defined by

$$\mathbf{J} = \begin{bmatrix} \frac{-1}{\sqrt{2}} & \frac{1}{\sqrt{2}} & 0 & \cdots & 0 \\ 0 & -1.0 & 1.0 & \ddots & \vdots \\ \vdots & \ddots & \ddots & \ddots & 0 \\ 0 & \cdots & 0 & -1.0 & 1.0 \\ 0 & \cdots & 0 & \frac{-1}{\sqrt{2}} & \frac{1}{\sqrt{2}} \end{bmatrix}. \quad (8)$$

Thus, we use $\|\mathbf{J}\mathbf{x}\|^2$ as the smoothness (and roughness) constraint.

Estimation Methods of Surface-Spectral Reflectance

A. Statistical Properties of Spectral Reflectance

We use a spectral reflectance database to obtain the statistical quantities of the surface-spectral reflectance \mathbf{x} such as the average \mathbf{x}_0 and the covariance \mathbf{P} . It should be noted that the ensemble average of surface-spectral reflectance is not zero because the spectral reflectance satisfies the condition $0 \leq x(\lambda_i) \leq 1$ ($i=1,2,\dots,N$). So, we set the average of \mathbf{x} as

$$\mathbf{E}[\mathbf{x}] = \mathbf{x}_0, \quad (9)$$

which has $\mathbf{x}_0 \geq \mathbf{0}$, and the covariance matrix of \mathbf{x} as

$$\mathbf{P} = \mathbf{E}[(\mathbf{x} - \mathbf{x}_0)(\mathbf{x} - \mathbf{x}_0)']. \quad (10)$$

B. PCA Method with Smoothness Constraint

When we suppose that a limited number of basis functions represents the spectral reflectance, the estimated spectral reflectance $\hat{\mathbf{x}}$ is described using the finite dimensional model as

$$\hat{\mathbf{x}} = \sum_{i=1}^K w_i \mathbf{b}_i + \mathbf{x}_0, \quad (11)$$

where \mathbf{b}_i ($i=1, 2, \dots, K$) are the basis vectors, representing the basis functions, and w_i are the weighting coefficients. The basis vectors are obtained from the principal components of a dataset consisting of many spectral reflectances. When the covariance matrix \mathbf{P} is decomposed into orthogonal components by using eigenvectors and eigenvalues, we have

$$\mathbf{P} = \mathbf{Q}\mathbf{\Lambda}\mathbf{Q}', \quad (12)$$

where $\mathbf{Q} = [\mathbf{q}_1, \mathbf{q}_2, \dots, \mathbf{q}_N]$ is an (N -by- N) matrix constructed with the eigenvectors \mathbf{q}_i ($i=1, 2, \dots, N$) and $\mathbf{\Lambda}$ is an (N -by- N) diagonal matrix constructed with eigenvalues λ'_i ($i=1, 2, \dots, N$), arranged in descending order as $\lambda'_i \geq \lambda'_{i+1}$. The basis vectors in Eq.(11) are then obtained as the K principal components taken from the first K eigenvectors $\mathbf{q}_1, \mathbf{q}_2, \dots, \mathbf{q}_K$. The principal components are also obtained from the spectral reflectance dataset's singular value decomposition (SVD).

Let $\mathbf{b}_i = \mathbf{q}_i$ ($i=1, 2, \dots, K$). The residual error of the observations is described as

$$\begin{aligned} \mathbf{y} - g\mathbf{A}\hat{\mathbf{x}} &= \mathbf{y} - g\mathbf{A}\mathbf{x}_0 - g\mathbf{A} \sum_{i=1}^K w_i \mathbf{b}_i \\ &= \mathbf{y}' - \mathbf{A}' \mathbf{w} \end{aligned} \quad (13)$$

where

$$\begin{aligned} \mathbf{y}' &= \mathbf{y} - g\mathbf{A}\mathbf{x}_0 \\ \mathbf{A}' &= [g\mathbf{A}\mathbf{b}_1, g\mathbf{A}\mathbf{b}_2, \dots, g\mathbf{A}\mathbf{b}_K] \\ \mathbf{w} &= [w_1, w_2, \dots, w_K] \end{aligned} \quad (14)$$

The term of smoothness constraint is described as

$$\begin{aligned} \mathbf{J}\mathbf{x} &= \mathbf{J} \left(\mathbf{x}_0 + \sum_{i=1}^K w_i \mathbf{b}_i \right) \\ &= \mathbf{J}\mathbf{x}_0 + \mathbf{B}' \mathbf{w} \end{aligned} \quad (15)$$

where

$$\mathbf{B}' = [\mathbf{J}\mathbf{b}_1, \mathbf{J}\mathbf{b}_2, \dots, \mathbf{J}\mathbf{b}_K]. \quad (16)$$

The present problem is to determine \mathbf{w} from a set of the observations. We solve this problem by minimizing the residual error and the roughness of the spectral reflectance based on the least-squares criterion. The cost function is then described as

$$L(\mathbf{w}) = \|\mathbf{y}' - \mathbf{A}' \mathbf{w}\|^2 + \mu \|\mathbf{J}\mathbf{x}_0 + \mathbf{B}' \mathbf{w}\|^2, \quad (17)$$

where μ is a weighting parameter for the roughness. When computing the derivative $\partial L / \partial \mathbf{w}$, the optimum \mathbf{w} to minimize L is given as a solution for the following equation.

$$-\mathbf{A}'' \mathbf{y}' + \mathbf{A}'' \mathbf{A}' \mathbf{w} + \mu \mathbf{B}'' \mathbf{J}\mathbf{x}_0 + \mu \mathbf{B}'' \mathbf{B}' \mathbf{w} = \mathbf{0}. \quad (18)$$

Therefore, the optimal weight \mathbf{w}_{opt} is determined as

$$\mathbf{w}_{\text{opt}} = \left(\mathbf{A}' \mathbf{A}' + \mu \mathbf{B}' \mathbf{B}' \right)^{-1} \left(\mathbf{A}' \mathbf{y}' - \mu \mathbf{B}' \mathbf{J} \mathbf{x}_0 \right). \quad (19)$$

The estimate of \mathbf{x} is finally obtained with \mathbf{w}_{opt} in the form

$$\hat{\mathbf{x}} = \sum_{i=1}^K w_{\text{opt},i} \mathbf{b}_i + \mathbf{x}_0. \quad (20)$$

C. LMMSE Method with Smoothness Constraint

The Wiener estimator of \mathbf{x} is sought in the form $\hat{\mathbf{x}} = \mathbf{B}\mathbf{y}$ to minimize the mean-square error (MSE) between the estimate $\hat{\mathbf{x}}$ and the original \mathbf{x} , that is $\mathbf{E} \left[\|\mathbf{x} - \hat{\mathbf{x}}\|^2 \right]$. On the other hand, the LMMSE estimate is sought in the more general form

$$\hat{\mathbf{x}} = \mathbf{B}\mathbf{y} + \mathbf{b}, \quad (21)$$

where \mathbf{B} is an (N -by- $3M$) matrix and \mathbf{b} is an N -dimensional constant vector. The optimal estimate is obtained as (see [10])

$$\hat{\mathbf{x}}_{\text{LMMSE}} = \mathbf{x}_0 + g \mathbf{P} \mathbf{A}' \left(g^2 \mathbf{A} \mathbf{P} \mathbf{A}' + a \mathbf{I} \right)^{-1} \left(\mathbf{y} - g \mathbf{A} \mathbf{x}_0 \right), \quad (22)$$

where a is the noise variance. The estimation error of the LMMSE estimator is always smaller than that of the Wiener estimator.

Now we consider the problem of minimizing the extended cost function with the smoothness constraint, which is described as

$$\begin{aligned} L(\mathbf{b}, \mathbf{B}) &= \mathbf{E} \left[\|\mathbf{x} - \hat{\mathbf{x}}\|^2 + \mu \|\mathbf{J}\hat{\mathbf{x}}\|^2 \right] \\ &= \mathbf{E} \left[\mathbf{x}' \mathbf{x} - 2\mathbf{x}' \hat{\mathbf{x}} + \hat{\mathbf{x}}' \left(\mathbf{I} + \mu \mathbf{J}' \mathbf{J} \right) \hat{\mathbf{x}} \right]. \end{aligned} \quad (23)$$

When we define

$$\tilde{\mathbf{x}} = \left(\mathbf{I} + \mu \mathbf{J}' \mathbf{J} \right) \hat{\mathbf{x}}, \quad (24)$$

the cost function is rewritten as

$$\begin{aligned} L(\mathbf{b}, \mathbf{B}) &= \mathbf{E} \left[\mathbf{x}' \mathbf{x} - 2\mathbf{x}' \left(\mathbf{I} + \mu \mathbf{J}' \mathbf{J} \right)^{-1} \tilde{\mathbf{x}} + \tilde{\mathbf{x}}' \left(\mathbf{I} + \mu \mathbf{J}' \mathbf{J} \right)^{-1} \tilde{\mathbf{x}} \right] \\ &= \mathbf{E} \left[\left(\tilde{\mathbf{x}} - \mathbf{x} \right)' \left(\mathbf{I} + \mu \mathbf{J}' \mathbf{J} \right)^{-1} \left(\tilde{\mathbf{x}} - \mathbf{x} \right) + \mathbf{x}' \left(\mathbf{I} - \left(\mathbf{I} + \mu \mathbf{J}' \mathbf{J} \right)^{-1} \right) \mathbf{x} \right]. \end{aligned} \quad (25)$$

It should be noted that the second term on the right-hand side in Eq.(25) is a constant vector, which is independent of \mathbf{b} and \mathbf{B} . The first term can be further rewritten using the trace of a square matrix as

$$\text{tr} \left\{ \left(\mathbf{I} + \mu \mathbf{J}' \mathbf{J} \right)^{-1} \mathbf{E} \left[\left(\tilde{\mathbf{x}} - \mathbf{x} \right) \left(\tilde{\mathbf{x}} - \mathbf{x} \right)' \right] \right\}. \quad (26)$$

The minimizer of $\mathbf{E} \left[\left(\tilde{\mathbf{x}} - \mathbf{x} \right) \left(\tilde{\mathbf{x}} - \mathbf{x} \right)' \right]$ in the sense of positive semi-definiteness minimizes Eq.(26). Because this estimate has no smoothness constraint, we have $\tilde{\mathbf{x}} = \hat{\mathbf{x}}_{\text{LMMSE}}$. Finally, from the definition in Eq.(24), we obtain the optimal estimate as

$$\hat{\mathbf{x}} = \left(\mathbf{I} + \mu \mathbf{J}' \mathbf{J} \right)^{-1} \hat{\mathbf{x}}_{\text{LMMSE}}. \quad (27)$$

Experimental Results

A. Experimental Setup

We conducted experiments using different mobile phone cameras to confirm the feasibility of the proposed methods in estimating the surface-spectral reflectance. Three mobile phone cameras were (1) Apple iPhone 6s, (2) Apple iPhone 8, and (3) Huawei P10 lite. The three mobile phone cameras' relative RGB spectral sensitivity functions are available at <http://ohlab.kic.ac.jp/>.

The camera images were captured in Adobe's digital negative (DNG) format, which is a lossless raw image format. The dark response was discarded from the camera output, so that the signal component represents a linear response to the input radiation. We used our own demosaicing algorithm to reconstruct a full-color image from the captured image. The bit depth of the cameras employed was 12 bits. The illumination light sources used in our experiments were seven ($M=7$) LED light sources. The spectral power distributions are shown in Figure 2. A spectral reflectance database was used to obtain the statistical quantities of the average reflectance \mathbf{x}_0 and the covariance \mathbf{P} , and the basis functions of spectral components of spectral reflectances. The database adopted was a data set of approximately 1500 spectral reflectances, which includes manmade objects such as papers, paints, and plastics as well as natural objects such as rocks, leaves, and skins.. All spectral functions were sampled at 5-nm intervals in the visible range (400–700 nm). Hence, we have $\Delta\lambda = 5$ and $N=61$.

Color samples from the X-Rite Color Checker Passport Photo were used to validate the reflectance estimation. Figure 3 (a) shows the imaging target comprising 24 color checkers and the white reference standard (Spectralon). Figure 3 (b) depicts the spectral reflectance values measured using a spectral colorimeter (CM-2600d, Konica Minolta).

The color images acquired under each illumination light were combined into a 21 channel multispectral image. The corresponding patch areas obtained multispectral observation data for each color patch. The gain parameter g and the noise variance a in the observation model were determined using the L1 norm minimizations based on the Spectralon data, according to the procedure shown in [10].

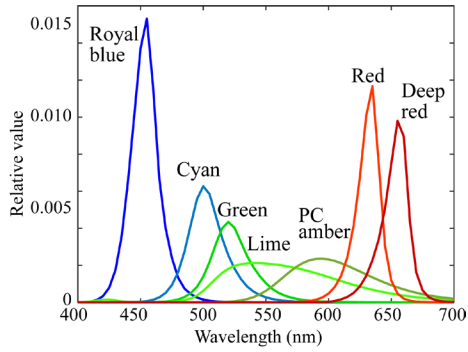


Figure 2 Spectral power distributions of seven LED light sources.

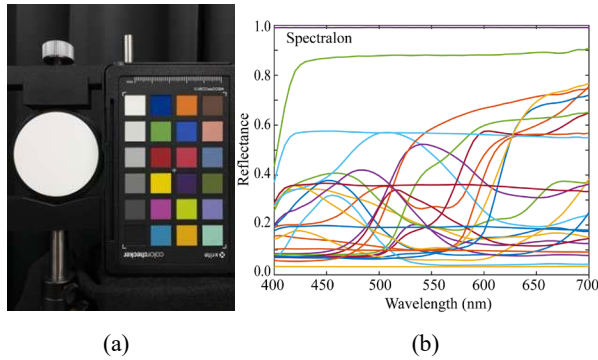


Figure 3 Color checkers adopted for reflectance estimation validation. (a) Imaging targets comprising 24 color checkers and the white reference standard (Spectralon). (b) Spectral reflectances of the 24 color checkers and the white reference standard measured by the spectral colorimeter.

B. Estimation Results

The accuracy of the estimated spectral reflectances was evaluated by the root-mean-square error (RMSE), calculated as the root of the average of the squared norm of the estimation errors per wavelength over the 24 color checkers. The RMSE calculation was changed from the calculation in [10]. Table 1 summarizes the performance values by the proposed methods for the spectral reflectance estimation, where the RMSE is presented for each case using the three mobile phone cameras. The PCA and LMMSE methods optimized with the smoothness constraint are compared, respectively, with the original PCA and LMMSE methods without the constraint.

The principal components in the PCA method were obtained from the SVD of the spectral reflectance data set. The first five principal components were selected as the basis functions, so that $K=5$ in Eq. (11) and Number of Bases=5. The errors in Table 1 were minimized using these basis functions. The PCA method may be easier than the LMMSE method because it does not require the parameter a of the noise variance. However, the PCA method was significantly less accurate than the LMMSE method as shown in Table 1. The parameter μ represents a weighting parameter for the roughness.

Table 1 shows that the spectral reflectances' estimation accuracies for all mobile phone cameras are improved by the proposed methods for PCA and LMMSE compared with the original methods. In particular, the improvement in the PCA method looks

more significant than that in the LMMSE method. However, it can be confirmed that the minimal RMSE among all methods is performed by the LMMSE method optimized with the smoothness constraint. Thus, the superiority of the proposed LMMSE method can be confirmed from the overall point of view.

We also evaluated the performance using the color difference. The CIE-LAB color differences under the illuminant D65 were calculated between the LAB coordinates based on the estimated spectral reflectance and the ones based on the directly measured spectral reflectance by a spectrometer, which was used as the ground truth. The CIE-LAB color differences when using iPhone 6s were $DE_{76}=5.49$ and $DE_{00}=2.76$ for the original LMMSE method without the constraint and $DE_{76}=4.82$ and $DE_{00}=2.56$ for the proposed LMMSE method with the smoothness constraint. Thus, the proposed method improved the color difference.

Table 1 RMSEs of the surface-spectral reflectances estimated via two methods, in which three different mobile phone cameras captured the 24 color checkers under 7 LED light sources.

Phone Model	RMSEs over 24 color checkers			
	PCA method optimized with smooth	PCA original method	LMMSE method optimized with smooth	LMMSE Original method
iPhone 6s	0.03583 N. bases=5 $\mu=45000$	0.04140 N. bases=5	0.03440 $\mu=2.0$	0.03472
iPhone 8	0.04062 N. bases=5 $\mu=200000$	0.04161 N. bases=5	0.03588 $\mu=1.0$	0.03597
Huawei P10 lite	0.04158 N. bases=5 $\mu=150000$	0.04267 N. bases=5	0.03962 $\mu=3.0$	0.04029

Conclusions

This paper considered the problem of estimating surface-spectral reflectance with a smoothness constraint from the image data. The measure of smoothness was defined to be the total variation of spectral reflectance, that is, the square of its derivative, integrated over the entire visible range. A penalty on the roughness of the spectral reflectance, equivalent to the smoothness constraint, is added to the performance index to estimate the spectral reflectance functions from image data. The optimal estimates of the spectral reflectance functions are determined to minimize a total cost function consisting of the estimation error and the roughness of the spectral functions.

First, we supposed a multispectral image acquisition system, where an RGB camera captures multiple images for the scene of an

object under multiple light sources. The observed image data were modeled using the spectral functions of spectral sensitivities, illuminant spectra, and unknown spectral reflectance also the two parameters of a gain and an additive noise term. Next, we developed the optimal estimation algorithms to minimize the total cost function for the two estimation methods of PCA and LMMSE. The optimal estimators for PCA and LMMSE were derived based on the least-square criterion and the mean squared error minimization criterion, respectively.

We experimented to confirm the feasibility of the proposed method using three mobile phone cameras and seven LED light sources. A spectral reflectance database was used to obtain the statistical quantities and the basis functions of spectral reflectance functions. The RMSEs evaluated the estimation accuracy for the test color checkers. We also showed the performance using the color difference. The proposed methods optimized based on the smoothness constraint improved the accuracy for both PCA and LMMSE estimators. Especially, the proposed LMMSE method was found to be the best in terms of estimation accuracy.

Acknowledgments

This work was supported by JSPS KAKENHI Grant Number JP 20K11877.

References

- [1] J. Cohen, Dependency of the spectral reflectance curves of the Munsell color chips, *Psychonomic Science*. Vol.1, pp.369–370 (1964).
- [2] L. T. Maloney, Evaluation of linear models of surface spectral reflectance with small numbers of parameters, *J. Optical Society of America A*, Vol. 10, pp.1673–1683 (1986).
- [3] J. P. S. Parkkinen, J. Hallikainen, and T. Jaaskelainen, Characteristic spectra of Munsell colors, *J. Optical Society of America A*, Vol. 6, 318–322 (1989).
- [4] L. T. Maloney and B. A. Wandell, Color constancy: A method for recovering surface spectral reflectance, *J. Optical Society of America A*, Vol. 3, pp. 29–33 (1986)
- [5] B.A. Wandell, The synthesis and analysis of color images, *IEEE Trans. Patt. Anal. Mach. Intell.*, Vol. 9, pp. 2–13 (1987).
- [6] S. Tominaga, Multichannel vision system for estimating surface and illuminant functions, *J. Optical Society of America A*, Vol.13, pp. 2163–2173 (1996).
- [7] C. van Trigt, Smoothest reflectance functions. I: Definition and main results, *J. Optical Society of America A*, Vol. 7, pp. 1891–1904 (1990).
- [8] C. van Trigt, Smoothest reflectance functions. II: Complete results, *J. Optical Society of America A*, Vol. 7, pp. 2208–2222 (1990).
- [9] C. Li and M.R. Luo, The estimation of spectral reflectance using the smoothest constraint condition, *Proc. IS&T/SID 9th Color Imaging Conference*, pp.62–67 (2001)
- [10] S. Tominaga, S. Nishi, R. Ohtera, H. Sakai, Improved method for spectral reflectance estimation and application to mobile phone cameras, *J. Optical Society of America A*, Vol. 39, pp.494–508, (2022).
- [11] F. H. Imai and R. S. Berns, Spectral estimation using trichromatic digital cameras,” *Proc. Inter. Sym. Multispectral Imaging. and Color Reproduction for Digital Archives*, pp. 42–49 (1999).
- [12] A. Mansouri, T. Sliwa, J. Y. Hardeberg, and Y. Voisin, “An adaptive-PCA algorithm for reflectance estimation from color images, *Proc. Inter. Conf. Pattern Recognition*, pp. 1–4 (2008).
- [13] X. Zhang and H. Xu, Reconstructing spectral reflectance by dividing spectral space and extending the principal components in principal component analysis, *J. Optical Society of America A*, Vol. 25, pp.371–378 (2008).
- [14] A. Mansouri, T. Sliwa, J. Y. Hardeberg, and Y. Voisin, Representation and estimation of spectral reflectances using projection on PCA and wavelet bases, *Color Research and Application*, Vol. 33, pp. 485–493 (2008).
- [15] H. Haneishi, T. Hasegawa, A. Hosoi, Y. Yokoyama, N. Tsumura, and Y. Miyake, System design for accurately estimating the spectral reflectance of art paintings, *Applied Optics*, Vol. 39, pp.6621–6632 (2000).
- [16] N. Shimano, Recovery of spectral reflectances of objects being imaged without prior knowledge, *IEEE Trans. Image Processing*, Vol. 15, pp.1848–1856 (2006).
- [17] P. Stigell, K. Miyata, and M. Hauta-Kasari, Wiener estimation method in estimating of spectral reflectance from RGB image, *Pattern Recognition and Image Analysis*, Vol. 17, pp. 233–242 (2007).
- [18] H. L. Shen, P.-Q. Cai, S.-J. Shao, and J. H. Xin, Reflectance reconstruction for multispectral imaging by adaptive Wiener estimation, *Optics Express*, Vol. 15, pp. 15545–15554 (2007).
- [19] P. Urban, M. R. Rosen, and R. S. Berns, A spatially adaptive Wiener filter for reflectance estimation, *Proc. 16th Color Imaging Conference*, pp. 279–284, (2008).
- [20] J. H. Yoo, D. C. Kim, H. G. Ha, and Y. H. Ha, Adaptive spectral reflectance reconstruction method based on Wiener estimation using a similar training set, *J. Imaging Science and Technology*, Vol. 60, 020503 (2016).
- [21] A. M. Nahavandi, Noise segmentation for improving performance of Wiener filter method in spectral reflectance estimation, *Color Research and Application*, Vol. 43, pp. 341–348 (2018).